AIP | Review of Scientific Instruments

A Mott polarimeter operating at MeV electron beam energies

V. Tioukine, K. Aulenbacher, and E. Riehn

Citation: Review of Scientific Instruments **82**, 033303 (2011); doi: 10.1063/1.3556593
View online: http://dx.doi.org/10.1063/1.3556593
View Table of Contents: http://scitation.aip.org/content/aip/journal/rsi/82/3?ver=pdfcov
Published by the AIP Publishing

A Mott polarimeter operating at MeV electron beam energies

V. Tioukine,[a] K. Aulenbacher, and E. Riehn
Institut für Kernphysik der Johannes Gutenberg-Universität Mainz D-55128 Mainz, Germany

(Received 20 October 2010; accepted 29 January 2011; published online 14 March 2011)

We have developed a Mott electron polarimeter for the Mainzer microtron (MAMI) accelerator in Mainz, Germany. At beam energies ranging between 1.0 and 3.5 MeV two double focusing magnet spectrometers collect elastically backscattered electrons from gold targets. In spite of the small spectrometer acceptance, a sufficient statistical efficiency is achieved to provide very fast measurements if beam currents typical for experiments at MAMI are being used. High reproducibility is achieved, demonstrating that the results of asymmetry measurements are independent of the primary beam current in a range from 0.004 to 45 μA at a level of $<1\%$ relative variation. Compared to low energy polarimeters of similar construction an improvement of a factor 2–3 in absolute accuracy seems possible. © *2011 American Institute of Physics*. [doi:10.1063/1.3556593]

I. INTRODUCTION

Elastic scattering in the Coulomb field of a nucleus provides one of the easiest means to analyze the spin-polarization (P) of an electron beam. Such "Mott polarimeters" are conceptually simple since they operate with an unpolarized target whereas other devices such as Møller[1]—or Laser Compton polarimeters[2] require double polarization experiments, i.e., with a spin-polarized target. A "standard" Mott polarimeter uses an electron beam of kinetic energy $E \approx 100$ keV and elastic scattering is detected by comparatively simple detectors such as surface barrier Si-diodes. Several experimental and theoretical difficulties limit the accuracy $\Delta P/P$ of such a standard Mott polarimeter[3] to about[4] 3%. A "retarding field"[5] Mott polarimeter with much better energy resolution overcomes some of the experimental obstacles and achieves accuracies between 1% and 2% if careful calibration procedures are followed.[6] Further improvement requires resort to much more sophisticated techniques such as double scattering experiments which can achieve accuracies[7,8] $< 0.5\%$.

In this paper we present a Mott polarimeter which is not fundamentally different from standard Mott polarimeters with respect to the scattering arrangement and experimental methods but makes use of beam energies in the range of 1.0–3.5 MeV. This is more than one order of magnitude larger than typical energies for Mott polarimeters. We discuss results which illustrate the following advantages for MeV–Mott polarimetry: First, MeV energies allow good reproducibility (Sec. III A) together with sufficiently high statistical efficiency in a range of beam currents that is well adapted to the needs of the experimental program at our accelerator (Sec. III B). Second, compared to low energies, targets of much higher surface density can be used, which makes the targets more robust and uniform. These advantages make the MeV–Mott polarimetry a very suitable instrument to monitor variations of the beam polarization with time. Furthermore, it was stated a long time ago[9] that standard Mott polarimeters operating at such high energies achieve an accuracy of polarization measurements in the range of 2%. In Sec. IV of this paper we revisit this claim in the light of advanced technical possibilities and come to the conclusion that an accuracy $\leq 1\%$ is in principle feasible.

A Mott experiment measures the experimental asymmetry

$$A_{\mathrm{exp}} = \frac{R\uparrow - R\downarrow}{R\uparrow + R\downarrow}, \tag{1}$$

with $R\uparrow$ ($R\downarrow$) representing the counting rates for spin up (down). With the exception of tiny parity violating effects which are negligible in our context, A_{exp} is only nonzero if a beam polarization component exists that is normal to the scattering plane.[10] Therefore, in a typical experiment, the polarization vector is oriented parallel to the normal direction. The analyzing power for single elastic electron scattering is usually called the "Sherman function," S_0, and depends on parameters such as scattering angle (θ), beam energy (E), and on the nuclear charge of the target material (Z). The behavior on S_0 vs θ is displayed for scattering on gold nuclei ($Z = 79$) for various energies in Fig. 1. The backscattering angle is fixed and chosen at 164°. The Sherman function S_0 at this angle is sufficiently large in the energy range from 1.0 to 3.5 MeV with a maximum at 2.0 MeV.

The Sherman function S_0 can be calculated theoretically and the relation between scattering asymmetry and analyzing power is then established by $A_0 = PS_0$. In experimental reality S_0 is changed to an "effective analyzing power," S_{eff}, for example, by the effects of multiple scattering in the target, hence $A_{\mathrm{exp}} = PS_{\mathrm{eff}}$. If there exists a means to determine S_{eff} (with some uncertainty ΔS_{eff}) the beam polarization is determined from

$$P = \frac{A_{\mathrm{exp}}}{S_{\mathrm{eff}}}. \tag{2}$$

The error ΔA_{exp} resulting from the measurement defined in Eq. (1) can become much smaller than ΔS_{eff}, the latter in consequence dominates the uncertainty of the polarization measurement.

Targets with high nuclear charge—typically Au with $Z = 79$—are used to maximize the analyzing power. The maximum value of Sherman function $S_{0,\mathrm{max}}$ increases with

[a]Electronic mail: tioukine@kph.uni-mainz.de.

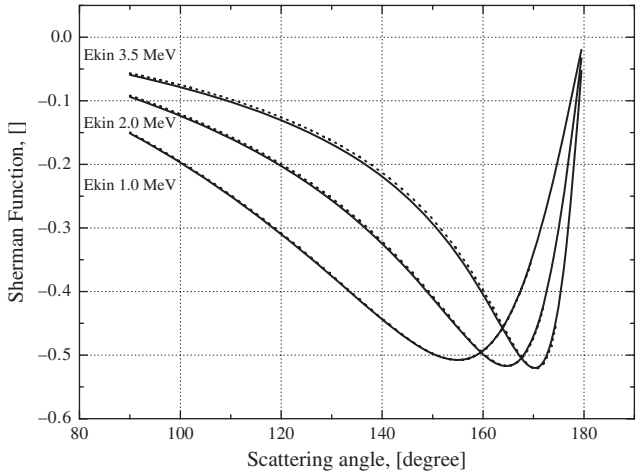

FIG. 1. Angular dependence of Sherman function for various energies (Z=79). Solid curves are for pure Coulomb potential, dotted ones for extended nucleus.

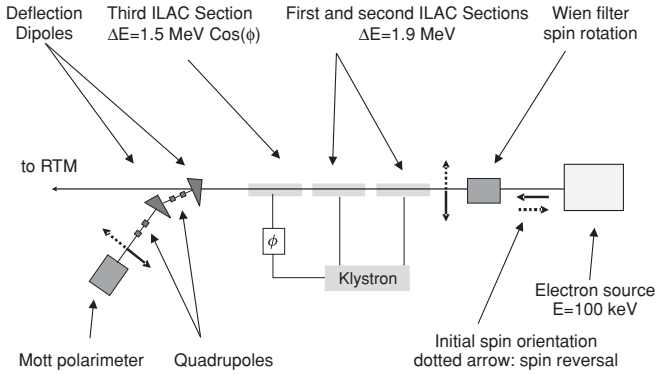

FIG. 2. Schematic layout showing installation of the Mott polarimeter at the 3.5 MeV injector of the MAMI RTM cascade. The beam energy can be changed by using a phase shifter (ϕ) in the waveguide between klystron and the third accelerating structure.

energy from 0.39 at 100 keV and $\theta = 120^\circ$ (Ref. 11) toward 0.55 at 3.5 MeV and $\theta = 170^\circ$. The gradual increase of $S_{0,\max}$ with energy appears to give an advantage. However, under laboratory conditions, this does not compensate for the technical effort to realize acceleration to energies much in excess of $\approx$ 120 keV. In addition, at high energies the angular region of large S_0 values becomes smaller and shifts toward extreme backward angles which reduces statistical efficiency (see Fig. 1). For this reason Mott polarimeters typically operate in a beam energy range between 20 and 120 keV. In this energy range, multiple scattering reduces S_{eff} strongly with target thickness. Therefore, extremely thin targets with surface densities $\mu < 100\,\mu\text{g/cm}^2$ are used which in turn requires using a low-Z backing material to provide a sufficient mechanical stability. Mott polarimeters of this kind have been a work horse for electron beam polarimetry for more than half a century. An excellent review is given in Ref. 6, the problems of thin target morphology and of the resulting uncertainties in the determination of S_{eff} are discussed in Ref. 12.

In this paper we describe a Mott polarimeter variant operating at the c.w. electron accelerator MAMI (Mainzer microtron) in Mainz, Germany. This accelerator consists of three cascaded race track microtrons (RTMs) which accelerate electrons to 855 MeV, followed by another stage, a harmonic double-sided microtron (HDSM), which allows for a maximum energy of 1.5 GeV.[13] The Mott polarimeter operates in the energy range between 1.0 and 3.5 MeV by using the output of the injector linear accelerator (ILAC) of MAMI (see Fig. 2).

II. APPARATUS

A. Electron beam

The Mott polarimeter is located behind the ILAC which provides 3.5 MeV kinetic beam energy in standard operation. This energy is required to make the beam sufficiently relativistic in order to inject it into the first RTM. The beam time structure is a c.w. sequence of electron pulses with 2.45 GHz repetition rate. Such a time structure is indistinguishable from dc for almost all particle detection systems since their signal bandwidth is much smaller than the pulse repetition rate. A schematic view of the injector part of MAMI is given in Fig. 2. A longitudinally polarized electron beam is produced in a 100 keV photoemission source.[14] Photoexcitation by circularly polarized laser light with a wavelength of $\lambda = 780$ nm shining on a GaAs/GaAsP superlattice photocathode[15] yields beam polarizations $P > 0.8$. A 180° flip of polarization—i.e., from spin up to spin down and vice versa—is provided by reversing the helicity of the laser light with a Pockels cell. After extraction of the longitudinally polarized electrons from the source, the polarization vector can be rotated by a Wien filter[16] into the transverse direction, which is required for a Mott asymmetry measurement. A rotation angle $\phi_{\text{Wien}} < 90^\circ$ reduces the Mott asymmetry according to $A = A_{\text{exp}}\sin(\phi_{\text{Wien}})$. The systematic studies presented in this article were all done with $\phi_{\text{Wien}} = 90^\circ$. The beam is accelerated in three radio frequency sections, the last section providing acceleration from 2 to 3.5 MeV. By varying the phase of the third section it is possible to diminish and even to partially reverse the acceleration process. This allowed us to vary the beam energy from 0.96 to 3.5 MeV. The relative beam energy stability, as measured with a magnetic spectrometer, is $\leq 5 \times 10^{-4}$.

For a polarization measurement the beam is guided to the polarimeter with the help of a magnet system consisting of two 15° bending dipoles. A quadrupole doublet which is centered around the midplane between the dipoles allows us to achieve optical properties similar to a Brown system.[17] The beam is focused onto the Mott-target in the polarimeter by a second quadruple doublet, a typical beam diameter on target is $\approx$ 1.5 mm. In contrast to low energy polarimeters, no diaphragms are used to define the beam reference line due to the high gamma ray background that could be introduced by such a measure. To provide reproducible alignment, the beam can be observed on several viewscreens (including the one at the Mott-target position) which yields a position reproducibility and pointing stability below 200 μm and < 2 mrad. If necessary, the beam position is corrected by small magnetic steering coils.

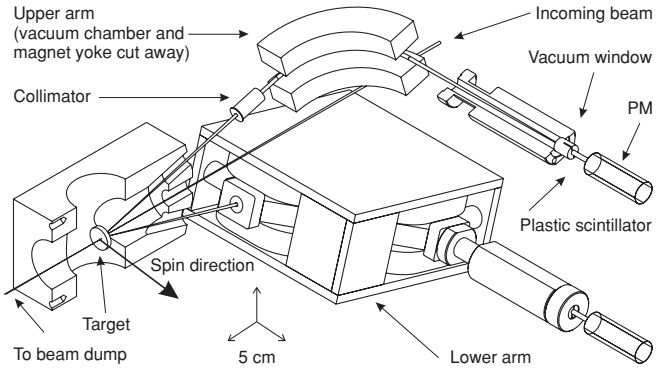

FIG. 3. Artists view of Mott polarimeter with magnetic spectrometers. Upward- or downward-scattered electrons are detected under $\theta = 164^\circ$. The observable polarization component is normal to the scattering plane. Upper magnet is partially removed for better visibility of electron trajectory. Shielding and 2 m long vacuum pipe to beam dump are not shown.

B. Polarimeter set-up

The polarimeter contains a set of gold targets of various thicknesses ($\approx$0.1, 0.25, 0.5, 1, and 15 μm corresponding to surface densities between $\mu = 0.2$ and $\mu = 30\,\mathrm{mg/cm^2}$) which are mounted in vacuum in a scattering chamber (Fig. 3). The targets are 16 mm in diameter and free standing (no backing); the three thinnest ones were fabricated at the target laboratory of the Gesellschaft für Schwerionenforschung (GSI) in Darmstadt, Germany. The target thickness is defined by α-absorption measurements with a relative error of about 3%. The two thickest targets are commercial products by Goodfellow, this manufacturer claims an accuracy of 15%. The target carrier also contains a viewscreen made from a Zn:S scintillator for visual beam inspection and an empty target holder for control of background conditions. The targets are moved into the beam by a linear motion vacuum feedthrough. The target chamber and all other vacuum parts are made from aluminum which reduces unwanted backscattering due to its low nuclear charge ($Z = 13$). Directly after the target chamber the beam tube diameter is increased to 100 mm to further reduce backscattering.

Since the polarization vector is in the horizontal plane, the scattering plane is chosen to be vertical. Two identical detection systems are used to detect electrons which are scattered upward or downward with respect to the horizontal plane. The scattering angle is 164° and remains fixed for all energies. Angular acceptance is defined by two circular 4 mm diameter collimators made from Al which are installed at a distance of 243 mm from the target. The collimators define an opening angle 16.5 mrad and a solid angle of 0.21 msr for each detector. The Sherman function for a finite acceptance must be calculated as cross-section weighted average over the acceptance, which therefore may differ from S_0 at 164°. The greatest sensitivity toward such an effect is found at 3.5 MeV where $dS/d\theta$ is maximized at 164°, whereas it would be minimized at 2.0 MeV where $dS/d\theta \approx 0$ (see Fig. 1). However, due to the very small acceptance this averaging does not lead to a significant variation with respect to S_0 at 164° even for 3.5 MeV. It should be noted that we have checked this only for single elastic scattering whereas in reality multiple scattering could create an even higher sensitivity which we plan to evaluate by Monte Carlo simulations of the backscattered intensity distribution in the future. The electrons passing the diaphragms enter double focussing spectrometer magnets which achieve stigmatic focusing by a suitably chosen magnetic field gradient.[18] The focal length is chosen to yield a 1:1 imaging of the beam spot on target to an image point behind the magnet where electron detection takes place by a cylindrical plastic scintillator of 10 mm diameter and 30 mm length. For different electron beam energies the bending radius in the magnets is kept constant by a suitable variation of the excitation current. Before reaching the scintillator the electrons leave the vacuum system by a 0.3 mm thick Al window. This comparatively thick material is chosen in order not to compromise the operational safety of the accelerator, since accidental venting due to a defective window could cause a long downtime of the accelerator complex.

The main purpose of the spectrometers is to remove the detectors from direct sight to the target, i.e., to reduce background from γ-rays which are amply produced by the electrons that are scattered to the chamber walls and from the beam dump. The scintillators are protected against such stray radiation by 10 cm thick lead shielding. The spectrometers are operated without slits, so that energy resolution is defined essentially by the size of the scintillator, which yields a FWHM resolution $E/\Delta E \approx 15$, whereas by using 1 mm wide slits in front of the scintillator it is possible to achieve a value greater than 100. Electrons reaching the detectors generate scintillation light which is converted into an electronic signal by photomultipliers.

C. Measurement procedure

The elastic count rate (R) is measured once per second. After each measurement the beam polarization is reversed. Since we employ two detectors (1,2) and polarization reversal ($\pm$) a ratio $Q = (R_1^+ R_2^-)/(R_1^- R_2^+)$ can be evaluated from two subsequent measurements. The experimental asymmetry can then be calculated from (Ref. 10)

$$A_{\mathrm{exp}} = \frac{1 - \sqrt{Q}}{1 + \sqrt{Q}}. \tag{3}$$

The advantage of this procedure is that apparative parameters which enter as a factor into the count rate but which are different for the two detector arms and/or the two measurement periods—such as detection efficiencies, solid angle, or unequal beam currents for the two helicity states—cancel when calculating Q. Otherwise, these nonsymmetrical parameters would create an apparative ("false") asymmetry. Whereas many causes for false asymmetries are removed by this technique, nonlinearities—e.g., dead time effects—are not. Fortunately, due to the high bandwidth of the plastic scintillator/photomultiplier arrangement we find negligible ($<1\%$) dead time effects for count rates $\leq$50 kHz which yields the typical count rate restriction for the experiments described below. In principle, much higher count rates can be tolerated, if a dead time correction scheme is applied.

An important purpose of the Mott polarimeter is to monitor long-term drifts of beam polarization since experiments at MAMI usually require run times of several weeks. In the majority of cases, the polarization measurements can be performed under the same conditions (e.g., beam current, spin rotation angle, see discussion in Sec. II A) as in operation for the experiment.

A set-up cycle in order to direct the beam to the Mott-target and to bring it back to a high energy physics experiment takes about 30 minutes. The main time-consuming factor is reoptimization of the injection into the accelerator stage RTM-1 which is probably caused by incomplete reproducibility of the beam trajectory due to remanence of the deflection magnet to the Mott polarimeter. The measurement time itself is almost negligible if compared to the beam cycle time. Due to the finite beam cycle time a reasonable period for monitor measurements is presently about once per day. This frequency can be increased to about once per hour if a deflector magnet with lower remanent field, as described in Ref. 19, would be installed. Routine measurements are guided by a semiautomatic procedure during which operator intervention is normally restricted to small corrections of the beam position on target. Automatic checks of the background conditions take place in order to warn against irregular operating conditions which could compromise reproducibility. For a given beam current and spin rotation angle the measurement continues until the desired statistical accuracy is achieved, afterward the beam is guided back to the experiment.

III. RESULTS

A. Stability and reproducibility

We checked for the stability of asymmetry measurements by performing a continuous series of measurements during a six hour long run which yielded 4500 asymmetries with an individual statistical accuracy of typically 1.5%. The distribution of asymmetries obtained (Fig. 4) is Gaussian with a variance that corresponds to the statistical accuracy of the single measurement. This excludes a drift of the results—i.e., limited stability of the apparatus on the time scale of the measurement—at a level of $< 0.1\%$.

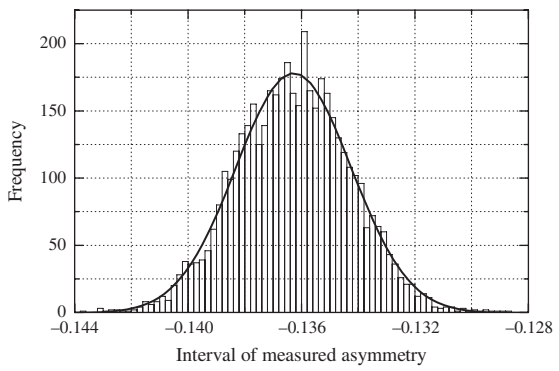

FIG. 4. Distribution of asymmetry values obtained by a series of asymmetry measurements. A Gaussian fit to the distribution has a variance of $\sigma = 0.002$ which is also the statistical uncertainty of the single measurement.

Additional variations of A_{exp} may be introduced by differing beam parameters after a new set-up of the polarimeter beam line. In order to estimate these variations we systematically changed beam parameters on a much larger scale than commonly encountered. For example, the beam was moved away from its reference position by ± 1 mm in both directions whereas the set-up procedure described above results in a position reproducibility of 0.2 mm. Similar tests were performed by varying the target position and the beam size. Even in extreme cases no relative variation of A_{exp} in excess of 1% was observed.

B. Statistical efficiency

The experimental asymmetry which was observed at various energies for the different targets yielded the curves displayed in Fig. 6, which demonstrates the decrease of effective analyzing power S_{eff} with target thickness. The values of S_{eff} quoted in this section were obtained from the relation $S_{\text{eff}}(d) = A_{\text{exp}}(d)/P$ by an independent measurement of P with a Møller polarimeter—see Sec. IV C. The error in S_{eff} is $\Delta S_{\text{eff}}/S_{\text{eff}} \approx 2\%$.

The statistical efficiency (figure of merit, FOM) of a polarimeter is commonly defined as

$$\text{FOM} = N S_{\text{eff}}^2 \frac{I_{\text{scat}}}{I_0}, \tag{4}$$

with I_{scat} and I_0 being the current recorded by the detector and the beam current respectively, $N = 2$ is the number of detectors. Given the fact that $S_{\text{eff}}(d)$ is of the same order of magnitude for all energies and since I_{scat} is roughly $\propto E^{-2}$ due to the energy dependence of the Mott cross-section it is evident that the FOM is larger for low energies, an expectation that was confirmed in our experiments. However, since the most important case from the point of view of support for the experiments at MAMI is the operation at 3.5 MeV, we will now focus on a discussion of statistical efficiency for this energy.

The scattered current can be obtained by inserting the target thickness d (in μm) and the beam current I_0 (in μA) in the relation $I_{\text{scat}} = k \cdot d \cdot I_0 \cdot e$ (e is the electron charge). If only single elastic scattering would be present, the factor k is a constant which can also be predicted from the material parameters, the cross section, and the angular acceptance of the detector system. This is the case for the three thinnest targets and the detected rates show agreement with the predicted value of k. For the two targets of largest thickness we observe a nonlinear increase—probably due to multiple scattering. The FOM [Eq. (4)] is then calculated for the individual targets by evaluating

$$\text{FOM} = 10^9 \, N \, e \, S_{\text{eff}}^2 \, k \, d.$$

The different target parameters are found in Table I. The reduction of S_{eff} with d is much less steep than at low energies; the 1 μm target, for example, still retains more than 80% of S_0. Compared to published values for 100 keV Mott polarimeters,[3] the thickness for the same relative reduction is larger by a factor of 40. This results in a sufficient mechanical stability of the targets, no target failures occurred during sev-

TABLE I. Efficiency parameters for the different targets at beam energy of 3.5 MeV and scattering angle $\theta = 164°$. The analyzing power for single elastic scattering is $S_0 = 0.459$.

d (μm)	Rate at 1 μA (kHz)	k (kHz/(μ m $\cdot$ μ A))	S_{eff}	FOM
0.10	0.17	1.7	0.447	0.11×10^{-10}
0.25	0.40	1.6	0.419	0.22×10^{-10}
0.50	0.80	1.6	0.398	0.44×10^{-10}
1.00	1.90	1.9	0.377	0.86×10^{-10}
15.00	50.00	3.3	0.161	4.08×10^{-10}

eral years of operation. In addition there is no need for target backing as it is required in the low energy apparatuses, where the resulting background must be carefully subtracted.

The FOM at 3.5 MeV is tiny if compared with that of low energy devices which may achieve[6] FOM $> 10^{-4}$, but it proves to be well adapted for the beam currents that are used for the experiments at MAMI. This can be visualized by observing that the 15 μm target yields 50 kHz count rate—the maximum which can be tolerated without dead time correction—at a beam current of 1 μA. For the given S_{eff} and typical beam polarizations of $P = 0.8$, this corresponds to a measurement time of ≈ 3 s for a relative statistical accuracy $\Delta A_{\text{exp}}/A_{\text{exp}} = 1\%$.

C. Measurements at different beam intensities

Experiments at MAMI require a wide range of beam intensities, ranging from 1 nA for experiments with circularly polarized γ-rays[20] to 30 μA which represents the limit for the liquid hydrogen targets presently available in our institute.[21] The Mott polarimeter allows us to measure with reasonable speed in the whole range. The results of such a measurement are shown in Fig. 5, each of the data points has a relative statistical accuracy $\approx 0.3\%$ which required less than two hours for the lowest current (4 nA).

The beam current was varied by passively attenuating the laser intensity in front of the input polarizer of the circular polarization optics at the polarized source. This avoids changes of laser wavelength or of the circular polarization which would otherwise change the beam polarization. All accelerator parameters remained fixed during the experiment. When the count rate approached the 50 kHz range we changed to a thinner target, several points were taken with the same current on two different targets to provide overlap. The results indicate that there is no dependence of polarization on the beam current at the given level of precision from 5 nA to 10 μA. A reduction of asymmetry by $\leq 1\%$ (relative) is visible at currents ≥ 10 μA. An explanation could be heating of the photocathode by the increased laser intensity. The finding of such a small variation of beam polarization with beam intensity is quite important for the experiments since absolute polarization measurements with the Møller polarimeter at MAMI can only be performed at very low currents ($\approx 50\,n$A).

IV. CALIBRATION OF THE MOTT POLARIMETER

The effective analyzing power of the targets was determined by the relation $S_{\text{eff}} = A_{\text{exp}}/P$. The beam polarization was measured by a calibrated Møller polarimeter which operates at the high energy end of the accelerator. Since the travel time of electrons in MAMI is very short (several microseconds) the spin transport can be modeled by computer-tracking of a representative beam-ensemble through the accelerator. The results exclude depolarization at a level $< 0.1\%$.[22] Furthermore, using the Wien filter spin rotator ensures the desired spin orientation at both polarimeters—transverse for the Mott, longitudinal for the Møller—with sufficient precision, making the contribution from angular errors negligible. Variations of the angle with time at the high energy end due to energy-dependent (g-2)-precession are excluded too, due to the high energy stability of the accelerator. Therefore, the uncertainty is dominated by the Møller calibration[23] resulting in $\Delta P/P \leq 2\%$.

It is desirable to achieve a "self-calibration" of the Mott polarimeter, i.e., without using an external apparatus. Self-calibration requires to determine the polarization from the relation $P = A_0/S_0$; in the first place it is necessary to extrapolate the observed asymmetries $A_{\text{exp}}(d)$ toward target thickness zero—yielding A_0. In addition, the single scattering analyzing power S_0 must be calculated. Both the determination of A_0 and S_0 introduce systematic errors. We address S_0 first.

A. Determination of S_0

Figure 1 presents the angular dependence of S_0 for various energies for a point charge together with values for an extended gold nucleus. These curves were obtained by using formulas given by Motz *et al.*[24] which allow solution of the Dirac equation with an arbitrary level of accuracy for scattering on a spherically symmetric potential. To test our calculations, we have checked them against published results[25] which we were able to reproduce. For 3.5 MeV the relative difference between point and finite nucleus is about 1% and it is even less for the lower energies. Contributions from the electron cloud are negligible for all energies. The reason for this insensitivity lies in the spacial resolution which corresponds to about 30 Fermi for the momentum transfer defined by 3.5 MeV and a scattering angle of 164°. This is much smaller than the typical extension of the electron cloud, but much larger than the nuclear radius. This behavior is in contrast to the situation at—and especially below—100 keV, where theoretical uncertainties are a limitation[11] even if all other effects would be under control. At high energies the uncertainty introduced by the unknown details of the structure—e.g., the nuclear radius—have therefore only a negligible influence ($< 0.5\%$) on the uncertainty in S_0. At even higher energies ($\gtrsim 10$ MeV) uncertainties caused by the nuclear structure will become more important.

Since our polarimeter operates with fixed scattering angle, $S_{0,\max}$ corresponds to the central detection angle (164°) exclusively at an energy of 2 MeV. For the other energies between 1 and 3.5 MeV $|S_0(\theta = 164°)|$ is still > 0.45. At energies different from 2 MeV, the slope of S_0 with angle creates some sensitivity toward position fluctuations on the target but these are well below 0.5% for the typical beam position reproducibilities.

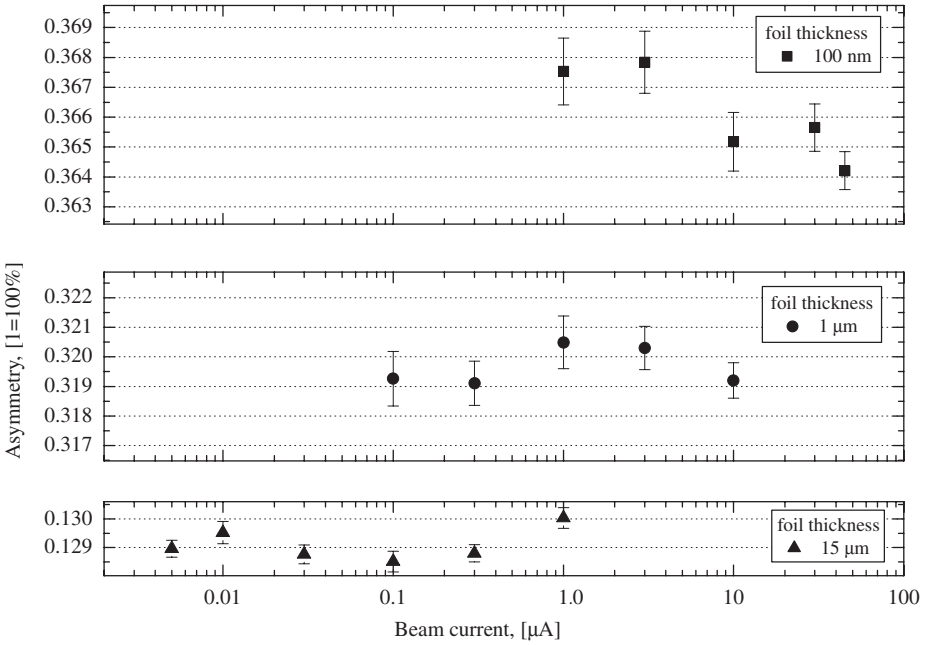

FIG. 5. Asymmetry vs beam current for various targets (statistical error bars).

In Fig. 7 we extract the beam polarization from the extrapolated A_0 (see below) and the value of S_0 taken from our calculations. The results are independent of beam energy with a variance of much less than 1%, which argue for the accuracy of S_0 calculations. Other error sources concerning S_0 are discussed in Sec. IV C.

B. Determination of A_0

Figure 6 presents experimental measured values of asymmetry $A_{\text{exp}}(d)$ for various targets at different beam energies. In order to make an extrapolation of $A_{\text{exp}}(d)$ toward A_0 a hypothesis for the dependence on the target thickness must be given. This must take into account the physical and apparative effects, assuming a constant beam polarization during the measurement.

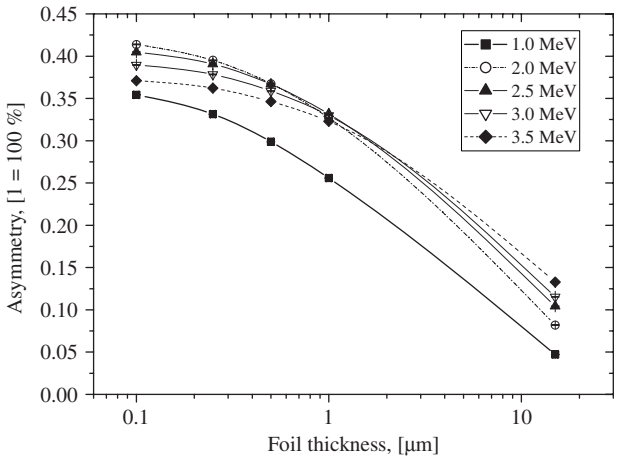

FIG. 6. Asymmetry vs foil thickness for various primary beam energies at a fixed scattering angle of 164°. Lines are "rational" fit functions (see text). The fits related to the "exponential" model have been omitted for better visibility.

The problem of finding a well motivated analytical form of $S_{\text{eff}}(d)$ is a difficult task and it is even more difficult to estimate the model dependent error if a specific method is chosen. However, as was noted by Gay,[12] the exact description is unimportant if the curvature of the true function is negligible at target thicknesses that are experimentally accessible. In this case a model function may fit the data and provide the same linear Taylor expansion as the true $S_{\text{eff}}(d)$, i.e., it will be exact since second order effects are supposed to be negligible by definition. It can be expected that the "linear regime" is easier to access for high energies due to the much larger target thickness required to obtain the same relative reduction of S_{eff}.

To which extent the linear regime is reached can be judged by choosing different fit functions and observing the variation of the predicted values A_0. In our case these variations are very small: We choose for example $A(d) = A_1 + A_2\exp(-kd)$ (initially proposed by Gay) and a second one, described by a ratio: $A(d) = A_1 + A_2/(1 + kd)$ which implicitly takes into account the polarization dependence of double scattering.[26] Both fit functions have three free parameters (A_1, A_2, k; different for each energy) and are equivalent with respect to their ability to fit the data. The difference in the two extrapolations is $\leq 0.6\%$ at energies ≥ 2 MeV (Fig. 7). This systematic error must be added linearly to all other errors, including the statistical error. The increased deviation at 1 MeV may be a result of larger nonlinearity of $S_{\text{eff}}(d)$ at this low energy. It therefore seems that nonlinearities do not contribute at the 1% level for energies ≥ 2 MeV and thicknesses of 100 nm.

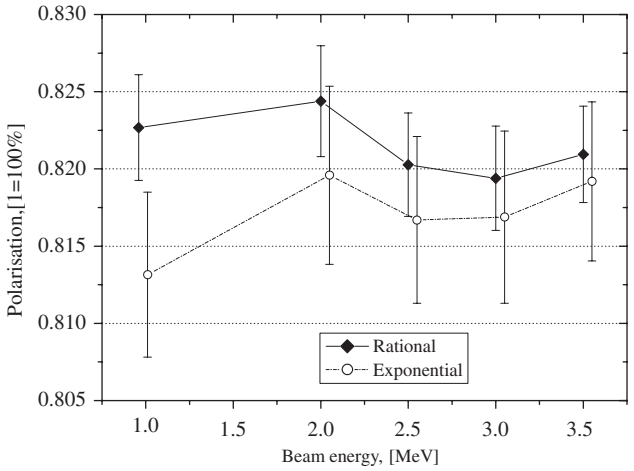

FIG. 7. Polarization determination for several energies using two different fit functions. Errors ($\pm 2\sigma$) are fit uncertainties only.

C. Remaining systematic errors: Status and future

We now discuss the potential improvement in the uncertainty of several parameters which currently limit the accuracy of the self-calibration.

S_0 : Radiative effects: So-called radiative effects may change the value of S_0. Though they are generally estimated to be $<1\%$ (Ref. 27), we are not aware of an existing quantitative calculation. We want to point out that the extraction $P = A_0(E)/S_0(E)$ in our experiment (Fig. 7) is energy independent within 0.6% at energies ≥ 2 MeV. Since radiative effects can be expected to be dependent on the momentum transfer (i.e., energy) there is indeed experimental support for the assumption that these effects are small. For the future we hope that a sound theoretical calculation can be made with a relative accuracy of 30% on this $O(1\%)$ contribution; hence, allowing to reduce the uncertainty below 0.5%.

S_{eff} : Extrapolation uncertainties: It was realized some years ago,[28] that modern computers allow to perform a Monte Carlo simulation of elastic multiple scattering without approximations. The method therefore provides an *ab initio* prediction of $S_{\text{eff}}(d)$ and eliminates the need for fit functions as they were used for extrapolation in Sec. IV B. We have already performed a feasibility study[29] which indicates that such a treatment is possible at MeV energies. It should be possible to determine the negative slope of $S_{\text{eff}}(d)$ with 10% accuracy in the thickness range between 0 and 100 nm. Since our experiments demonstrate that the overall relative reduction of S_{eff} for this thickness cannot be much larger than $\approx 3\%$—see Table I—the error in slope will only cause an error of 0.3% in S_{eff}(100nm). The error induced by the 3% error in target thickness is even smaller.

A_{exp} : Target induced background: A background which reduces A_{exp} can be created by the electrons which are scattered from the vacuum chamber wall after forward scattering in the target and are then detected, or create γ-radiation which penetrates the detector shield. However, the contribution from such a background is certainly small because we observe that the polarization values which are obtained by evaluating $P = A_0/S_0$ (Fig. 7)—without any background subtraction—are lower than the Møller values only by 4%. It is possible to quantify the contribution of such a background, for example, by simulations which take into account geometry and material. Furthermore, apparatus improvement is possible by introducing carbon or beryllium lining in the scattering chamber to reduce both backscattering and γ-ray production. We therefore hope to be able to control the contribution of backgrounds to A_{exp} at the $< 0.5\%$ level.

V. CONCLUSION

The 3.5 MeV Mott polarimeter offers high measurement speed and good reproducibility ($\Delta A_{\text{exp}}/A_{\text{exp}} < 0.01$) of results. This is the case for almost all beam intensities that are presently in use for hadron physics experiments at the MAMI accelerator. For this reason the device is well suited for polarization monitoring in long-term experiments. The demonstrably small dependence of analyzing power on target thickness and the consistent results that are achieved over a wide energy range allow to address the systematic error sources at individual accuracy levels of $<0.5\%$. This may finally lead to an overall accuracy of $\leq 1\%$.

ACKNOWLEDGMENTS

This work was supported by the SFB 443 of the Deutsche Forschungsgemeinschaft and by the Bundesministerium für Bildung und Forschung within project 05H10UME "Spin management." We want to thank Dr. Bettina Lommel from GSI for providing us with the free standing gold targets and the A1 collaboration at MAMI for the Møller measurements and productive discussions.

[1] M. Hauger, A. Honegger, J. Jourdan, G. Kubon, T. Petitjean, D. Rohe, I. Sick, G. Warren, H. Wöhrle, J. Zhao, R. Ent, J. Mitchell, D. Crabb, A. Tobias, M. Zeier, and B. Zihlmann, Nucl. Instrum. Methods Phys. Res. A **462**, 382 (2001).
[2] ALEPH, DELPHI, L3, OPAL and SLD Collab., Phys. Rep. **427**, 257 (2006).
[3] G. D. Fletcher, T. J. Gay, and M. S. Lubell, Phys. Rev.A **34**, 911 (1986).
[4] Throughout this paper we have quoted absolute values of polarization observables by a dimensionless number, whereas all accuracies are relative ones ($\Delta P/P$, $\Delta A/A$, etc.) and are given in percent units.
[5] L. A. Hodge, T. J. Moravec, F. B. Dunning, and G. K. Walters, Rev. Sci. Instrum. **50**, 5 (1979).
[6] T. J. Gay and F. B. Dunning, Rev. Sci. Instrum. **63**, 1635 (1992).
[7] A. Gellrich and J. Kessler, Phys. Rev. A **43**, 204 (1991).
[8] S. Mayer, T. Fischer, W. Blaschke, and J. Kessler, Rev. Sci. Instrum. **64**, 952 (1993).
[9] A. R. Brosi, A. I. Galonsky, B. H. Ketelle, and H. B. Willard, Nucl. Phys. **33**, 353 (1962).
[10] J. Kessler, *Polarized Electrons Series on Atoms and Plasmas*, 2nd ed. (Springer, New York, 1985).
[11] A. W. Ross and M. Fink, Phys. Rev. A **38**, 6055 (1988).
[12] T. J. Gay, M. A. Khakoo, J. A. Brand, J. E. Furst, W. V. Meyer, W. M. K. P. Wijayaratna, and F. B. Dunning, Rev. Sci. Instrum. **63**, 114 (1992).
[13] K.-H. Kaiser, K. Aulenbacher, O. Chubarov, M. Dehn, H. Euteneuer, F. Hagenbuck, R. Herr, A. Jankowiak, P. Jennewein, H.-J. Kreidel, U. Ludwig-Mertin, M. Negrazus, S. Ratschow, St. Schumann, M. Seidl, G. Stephan, and A. Thomas, Nucl. Instrum. Methods Phys. Res. **593**, 159 (2008).
[14] K. Aulenbacher, Ch. Nachtigall, H. G. Andresen, J. Bermuth, Th. Dombo, P. Drescher, H. Euteneuer, H. Fischer, D. v. Harrach, P. Hartmann, J. Hoffmann, P. Jennewein, K.-H. Kaiser, S. Köbis, H. J. Kreidel, J. Langbein, M. Petri, S. Plützer, E. Reichert, M. Schemies, H.-J. Schöpe, K.-H. Steffens, M. Steigerwald, H. Trautner, and Th. Weis, Nucl. Instrum. Methods Phys. Res. A **391**, 498 (1997).

[15]T. Maruyama, D.-A. Luh, A. Brachmann, J. E. Clendenin, E. L. Garwin, S. Harvey, J. Jiang, R. E. Kirby, C. Y. Prescott, R. Prepost, and A. M. Moy, Appl. Phys. Lett. **85**, 2640 (2004).
[16]V. Tioukine and K. Aulenbacher, Nucl. Instrum. Methods in Phys. Res. A **568**, 537 (2006).
[17]S. Penner, Rev. Sci. Instrum. **32**, 150 (1961).
[18]D. L. Judd, Rev. Sci. Instrum. **21**, 213 (1950).
[19]H. Euteneuer, H. Herminghaus, K. W. Nilles, and H. Schöler, *Proceedings 1st European Particle Accelerator Conference, (EPAC88)*, edited by S. Tazzari (World Scientific, Singapore, 1989), p. 1149.
[20]J. Ahrens, S. Altieri, J. R. M. Annand, G. Anton, H.-J. Arends, K. Aulenbacher, R. Beck, C. Bradtke, A. Braghieri, N. Degrande, N. d'Hose, H. Dutz, S. Goertz, P. Grabmayr, K. Hansen, J. Harmsen, D. von Harrach, S. Hasegawa, T. Hasegawa, E. Heid, K. Helbing, H. Holvoet, L. Van Hoorebeke, N. Horikawa, T. Iwata, P. Jennewein, T. Kageya, B. Kiel, F. Klein, R. Kondratiev, K. Kossert, J. Krimmer, M. Lang, B. Lannoy, R. Leukel, V. Lisin, T. Matsuda, J. C. McGeorge, A. Meier, D. Menze, W. Meyer, T. Michel, J. Naumann, R. O. Owens, A. Panzeri, P. Pedroni, T. Pinelli, I. Preobrajenski, E. Radtke, E. Reichert, G. Reicherz, Ch. Rohlof, D. Ryckbosch, F. Sadiq, M. Sauer, B. Schoch, M. Schumacher, B. Seitz, T. Speckner, M. Steigerwald, N. Takabayashi, G. Tamas, A. Thomas, R. van de Vyver, A. Wakai, W. Weihofen, F. Wissmann, F. Zapadtka, and G. Zeitler, Phys. Rev. Lett. **87**, 022003 (2001)
[21]S. Baunack, K. Aulenbacher, D. Balaguer Rios, L. Capozza, J. Diefenbach, B. Glöser, D. von Harrach, Y. Imai, E.-M. Kabuß, R. Kothe, J. H. Lee, H. Merkel, M. C. Mora Espi, U. Müller, E. Schilling, G. Stephan, C. Weinrich, J. Arvieux, M. A. El-Yakoubi, R. Frascaria, R. Kunne, F. E. Maas, M. Morlet, S. Ong, J. van de Wiele, S. Kowalski, Y. Prok, and S. Taylor, Phys. Rev. Lett. **102**, 151803 (2009).
[22]Ch. Nachtigall, E. Reichert, M. Schemies, M. Steigerwald, K. Aulenbacher, H. Euteneuer, D. v. Harrach, P. Hartmann, P. Hoffmann, P. Jennewein, K.-H. Kaiser, H. J. Kreidel, M. Leberig, J. Schuler, and Ch. Zalto, in *Proceedings 6th European Particle Accelerator Conference, (EPAC98)*, edited by S. Myers (Institute of Physics, University of Reading, Berkshire, 1998) p. 1430.
[23]P. Bartsch, D. Baumann, J. Bermuth, R. Böhm, K. Bohinc, D. Bosnar, M. Ding, M. Distler, D. Drechsel, D. Elsner, I. Ewald, J. Friedrich, J. M. Friedrich, S. Grözinger, S. Hedicke, P. Jennewein, M. Kahrau, S. S. Kamalov, F. Klein, K. W. Krygier, A. Liesenfeld, H. Merkel, P. Merle, U. Möller, R. Neuhausen, Th. Pospischil, M. Potokar, G. Rosner, H. Schmieden, M. Seimetz, A. Söle, L. Tiator, A. Wagner, Th. Walcher, and M. Weis, Phys. Rev. Lett. **88**, 142001 (2002).
[24]J. W. Motz, H. Olsen, and H. W. Koch, Rev. Mod. Phys. **36**, 881 (1964).
[25]P. Ugincius, H. Überall, and G. H. Rawitscher, Nucl. Phys. A **158**, 418 (1970).
[26]H. Wegener, Z. Phys. **151**, 252 (1958).
[27]J. M. Grames, C. K. Sinclair, J. Mitchell, E. Chudakov, H. Fenker, A. Freyberger, D. W. Higinbotham, M. Poelker, M. Steigerwald, M. Tiefenback, C. Cavata, S. Escoffier, F. Marie, T. Pussieux, P. Vernin, S. Danagoulian, V. Dharmawardane, R. Fatemi, K. Joo, M. Zeier, V. Gorbenko, R. Nasseripour, B. Raue, R. Suleiman, and B. Zihlmann, Phys. Rev. ST Accel. Beams. **7**, 042802 (2004).
[28]M. A. Khakoo, D. Roundy, C. Hicks, N. Margolis, E. Yeung, A. W. Ross, and T. J. Gay, Phys. Rev. A **64**, 052713 (2001).
[29]K. Aulenbacher and V. Tioukine, in *Proceedings 18th International Spin Physics Symposium, Charlottesville, VA (USA)*, edited by D. G. Crabb, Y. Prok, M. Poelker, S. Liuti, D. B. Day, and X. Zheng (AIP, Melville, New York, 2008), p. 1155.